 DOI: 10.1002/masy.201050813

Development of Nanocomposite Scaffolds for Bone Tissue Engineering

H.R. Imam Khasim,[*1] *S. Henning,*[2] *G.H. Michler,*[2] *Joerg Brand*[3]

Summary: Nanocomposite scaffold materials based on biodegradable polymers, as there are poly(3-hydroxybutyrate (PHB), poly(hydroxybutyrate-*co*-hydroxyvalerate) (PHBHV) and polycaprolactone (PCL), and nanocrystalline hydroxyapatite (HA) have been developed for the application as biomimetic bone substitution materials and materials for the tissue engineering of bone. Parameters like pore size, shape and interconnectivity are optimized to facilitate the formation of new bone. In this paper we describe a manufacturing method for compact nanocomposite scaffolds as well as for 3-dimesional porous scaffolds. Nanocomposite scaffolds consisting of PHB and HA needles or PHBHV and HA spheres, respectively, exhibit a very good filler dispersion even at 20 wt% loading. Smaller nanoparticles (needles) slightly tend to develop more agglomerates due to higher van der Waals forces of attraction compared to the larger spherical nanoparticles which were more uniformly dispersed. To produce porous structures, templates consisting of sugar and NaCl grains of varying grain size were used. In freeze-drying and particulate leaching processes smaller grain sizes resulted in pores with 46 to 70 μm, whereas grain sizes of more than 400 μm resulted in pores with 300 to 600 μm in diameter. The application of polymer solutions with a concentration of 5% (w/v) resulted in larger pore sizes compared to solutions of 10% (w/v). By the application of the melt infiltration technique to PCL, the resulting pore size was less influenced by the concentration of the polymer solution. It can be demonstrated that these techniques are suitable for the fabrication of nanocomposite scaffolds with uniform filler dispersion and porosity up to 98%.

Keywords: bone substitute; hydroxyapatite; nanocomposite, poly(3-hydroxybutyrate); tissue engineering

Introduction

There is a steadily increasing number of biomaterials that are used routinely in medical applications such as controlled drug release, hip and knee arthroplasty, device based therapies, medical imaging, and so on.[1] Since long it is recognized that the material properties affect biological outcomes including the half-life of drugs, biocompatibility of implanted devices, and release rates and toxicity of drug carriers.[2,3] Similarly, properties of biomaterials can have a profound impact on cell proliferation and remodeling of tissues.[4] The challenge that has fascinated material scientist from the beginning has therefore been how to design and control material properties to achieve a specific biological response. For example, the fabrication of 3-dimensional interconnected porous structures can facilitate cells to proliferate inside the substrates, and the incorporation of bioactive fillers and proteins can enhance tissue growth rate. Methods have been

[1] Translational Centre for Regenerative Medicine, University Leipzig, Philipp-Rosenthal-Str.35, D-04103, Leipzig, Germany
E-mail: hadimani@rz.uni-leipzig.de
[2] Institute of Physics, Martin Luther University Halle-Wittenberg, D-06099 Halle (Saale), Germany
[3] Department of Orthopaedics, Martin Luther University Halle-Wittenberg, Magdeburger Str. 22, 06097 Halle (Saale), Germany

developed for fabricating polymeric particles with controlled shape[5,7] mechanical properties[8,9] surface topology and compartmentalization.[10] Mechanical propertiesof the substrate have been demonstrated to produce a profound impact on cell and tissue behavior.[11] Mechanical properties of composites can be modified by adding filler particles to polymer matrix.[12] More over many of mechanical parameters depend on the filler dispersion in the matrix and the distance between the interphases. A special issue is the development of materials for regeneration of bone and bone tissue engineering because here the mechanical properties of the biomaterial are of outstanding significance. The incorporation of HA filler into a polymer matrix will combine the osteoconductivity of HA with the good mechanical and processing properties of polymers. Moreover, the combination of mechanical and biological features of polymeric and ceramic components offers the possibility to design composites with matching properties, such as degradability with controlled rate and superior mechanical properties like toughness and stiffness. The evolution from conventional particulate-filled systems to nanocomposites may help to solve the problem of embrittlement that occurs at higher filling ratios and lack of filler-matrix adhesion.

Another implication of fabrication in tissue engineering are three-dimensional biodegradable polymeric scaffolds which play an important role as biologically active, temporary supports for the transplantation of specific cells and tissues. Besides biocompatibility, biodegradability, processability, sterilizability, and mechanical strength of the scaffolding material, careful design of the microstructure and morphology of the porous structures is of critical importance for their success. In general a high porosity and a high interconnectivity of these scaffold is desired to minimize the amount of implanted polymer and to increase the specific surface area for cell attachment and tissue ingrowth. Furthermore, the pore morphology can affect the growth of cells and even alter cell function.[13] Interconnected pores larger than the dimensions of the cells are essential for allowing infiltration of the cells into the scaffold, whereas smaller pores may positively influence the exchange of nutrients and cellular waste products.[14] Therefore, an appropriate pore size range and distribution of pore sizes is beneficial to the viability and function of the cells within the tissue-engineering scaffolds.

Various methods have been used for the preparation of porous polymeric structures for biomedical applications and tissue engineering. Techniques involving phase inversion processes such as liquid–liquid phase separation and liquid–solid phase separation have been explored.[15] Freeze-drying has also been used frequently in the preparation of porous polymeric structures.[16] Morphology and properties of the resultant scaffolds largely depend on the phase separation mechanism.[17] In methods based on the leaching of soluble particulates[18,19] the porosity can be effectively controlled by variation of the amount of leachable particles, and the pore size of the porous structure can be adjusted independently of the porosity by using particles of different sizes. To improve the pore interconnectivity of the scaffold, particulate leaching has been used in combination with gas foaming,[20] solvent casting,[21,22] freeze-drying,[23,24] immersion precipitation,[25,26] coprecipitation[26] and compression molding.[19]

In this work we have used bacterial poly(3-hydroxybutyrate) (PHB) polyester which was derived from microorganisms was chosen for its hydrophobicity and thermoplastic nature.[27,29] Since it is enzymatically synthesized, it has exceptional stereochemical purity and as a consequence the polymer is completely isotactic and can crystallize and hydroxyapatite as inorganic filler for its good osteoconductive and osteoinductive properties. Emphasis is given on the fabrication of different kind of scaffolds (two and three dimensional) that could be used in different tissue engineering applications with the target application in bone tissue engineering.

Experimental Part

Materials

Poly(3-hydroxybutyrate) (PHB) ($M_n \approx$ 2,000,000 g/mol) was obtained from the methanotrophic strain Methylocystis sp. GB 25 DSMZ 7674 under non-sterile conditions in a bioreactor (Umweltforschungszentrum Leipzig, Germany). The obtained polymer is highly crystalline with high stereochemical purity and a glass transition temperature of $T_g = 5\,^{\circ}C$. Commercial grade poly(3-hydroxybutyrate) with $M_n = 440{,}000$ g/mol was purchased from BIOMER Krailling, Germany. PHBHV copolymer with a hydroxyvalerate (HV) comonomer content of 12% and poly(ε-caprolactone) (PCL with $M_n =$ 2000 g/mol) were obtained from Sigma-Aldrich, Germany. Two different types of nanofillers were used. OSTIM® medical grade nanocrystalline hydroxyapatite (needles) was purchased from Heraeus, Germany. Hydroxyapatite nanopowder (spherical particles) was obtained from Aldrich, Germany. Ethanol and chloroform of analytical grade were purchased from Carl Roth GmbH, Germany. Commercial food quality sugar cubes ($27.5 \times 18 \times 12$ mm, bulk density 1.007 g/cm^3, porosity 36.5%) were used as sucrose templates. Alternatively, sugar or sodium chloride templates were prepared by fusing sugar or salt particles (NaCl, cell culture grade, Roth, Germany). The particles were sieved with standard testing sieves (ASTM–11 specification) with mesh sizes of 200, 300 and 500 μm.

Preparation of Compact Composite Films

Pure polymer films were obtained by solution casting and subsequent solvent evaporation. Nanocomposites with 5, 10, 15 and 20 wt% hydroxyapatite filler content were produced by mixing appropriate amounts of a suspension of nanocrystalline HA in ethanol and a dilute solution of the polymer using $CHCl_3$ as solvent. The process is supported by ultrasonification (Vibrosonic Sonicator). The resulting nanocomposite solution was poured into a petri dish and the solvent was evaporated at room temperature. Subsequently, the nanocomposite films were vacuum dried for 24 h to remove the residual solvent. To produce larger films of a defined thickness, the nanocomposite solutions were cast on a glass plate using a film applicator (ELCOMETER 3570) or by means of a laboratory glass rod with custom-made spacers.

Pre-Fabrication of Sugar and Salt Templates

Salt granules were finely powdered using a laboratory high speed mixer (Analysenmühle A10, Janke&Kunkel GmbH). Subsequently, the powder was sieved using different mesh sizes to select defined grain sizes. The powders were pressed into autoclavable PTFE O-rings with a diameter of 5 mm and a height of 2 mm and fused following a procedure suggested by Feijen et al.[21,25] Sugar or salt particles of a defined size range were first soaked in a mixture of acetone and water and than gently packed into the PTFE rings. After drying, they were transferred into desiccators with relative humidity of 75% for 2 days. Finally, the templates were removed from the rings.

Preparation of Porous Polymeric Structures by a Combination of Freeze-drying and Particulate Leaching

The polymer (PHB or PCL, respectively) was dissolved in chloroform at 48 °C in order to achieve a 10% (w/v) solution. The nanocomposite solution was prepared in the same manner as described for the compact films. The pre-designed sugar or salt templates were dipped into the nanocomposite solution and fixed to a Rotavapor R-210 rotary evaporator equipped with vacuum pump. Vacuum was applied repeatedly by varying the pressure in between 200-350 mbar for a period of 1 hour. Subsequently the sugar / salt templates in which polymer was forced to penetrate were frozen using liquid nitrogen for few minutes and then transferred to deep freezer maintained at −80 °C for 24 h. After phase separation, the solvent

crystals were removed by freeze-drying for a period of 2–3 days in vacuum using ALPHA 1-4 LSC at a vacuum of 0.04 mbar and a temperature of −61 °C. Subsequently the structures were gently stirred in demineralized water with changing the water three times a day for about a week to leach out the sugar/salt. Finally, the resulting 3-dimensional porous nanocomposite scaffolds were dried in vacuum.

Preparation of Porous Scaffolds using Melt Infiltration Technique

The PCL polymer was melted at 60 °C. After adding hydroxyapatite nanoparticles the mixture was sonicated for a few minutes to disperse the filler uniformly. The suspension was poured into a metal mold containing commercially available sugar templates preheated to 60 °C using a vacuum drying chamber (MEMMERT PM 200). To force the melt to penetrate the pores of the template, vacuum was applied repeatedly in the range between 50 to 15 mbar. After complete solidification, the PCL/HA composites were removed, and the sugar particles were leached out in demineralized water for one week.

Scanning Electron Microscopy (SEM)

Scanning electron micrographs were obtained using a JEOL JSM 6300 SEM operated at 15KV. The surface morphology of compact films was investigated for all composites. To study the morphology of porous scaffolds, samples were quenched in liquid nitrogen and cut using a disposable metal blade. All samples were coated with a 10 nm gold layer (EDWARDS sputter coater).

Transmission Electron Microscopy (TEM)

Ultrathin sections of solution-cast samples were produced by means of a LEICA Ultracut cryo-ultramicrotome equipped with a DIATOME diamond knife. The sections were stained with ruthenium tetroxide (RuO_4) vapor for 4 h at room temperature and examined using a LEO 912 EFTEM transmission electron microscope.

Determination of Porosity

Density and porosity of the scaffolds were determined in triplicate by measuring the dimensions and the mass of the scaffold. The density (d) of the scaffolds was calculated as follows

$$d = \frac{m}{v} \tag{1}$$

where m is the mass and v is the volume. The porosity p_o was calculated as

$$P_0 = 1 - \frac{d}{d_p} \tag{2}$$

where d_p is the density of the nonporous compression moulded polymer also determined from the specimen mass and volume ($d_p = 1.246 \pm 0.009$ and 1.2368 ± 0.008 g/cm^3 for PHB and PCL, respectively).[30]

Results and Discussion

Morphology of Compact Nanocomposite Films

The uniform dispersion of nanoparticles in a polymeric matrix is a general technical problem, especially if one is considering higher filler content. On one hand, there exist van der Waals forces of attraction between the particles that are important in the process of particle agglomeration. On the other hand, polymer viscosity plays a significant role to achieve good dispersion. Here, dilute solutions with a concentration of 5% v/v were used. As we know in nanotechnology that the ultimate mechanical properties are also influenced by the morphology that develops while fabricating. To optimize the dispersion the sonication time was varied from 0 to 90 min. The best result was obtained using a total mixing time of 30 min. Further increment of dispersion time increases the temperature of the polymer solution and inturn increases the viscosity. At higher viscosities the movement of the chains is restricted and this will also decrease the nanoparticle movement ie the nanoparticles should overcome the van der Waals forces to separate itself and then it should overcome

the movement of restricted chains. Transmission electron microscopy (TEM) analysis was conducted to verify the size and dispersion quality of the nanocomposite. Figure 1a is the TEM image of a PHB/HA (90/10) nanocomposite. The nanoparticles are needle shaped with an average diameter of 18-30 nm. It can be observed that the particles are effectively dispersed. However, there is some residual agglomeration of particles in the range of 30–50 nm. Figure 1b is the TEM image of PHB/HA (80/20) wt% nanoparticles. Here also we can observe very good dispersion of the particles but with the number of agglomerated particles seems to be increased. This increasing in filler loading creates non-uniformity that is clearly observed in TEM. However filler loading of less than 2% gives better dispersion and homogeneity.

Size effect of nanoparticle also plays an important role for uniform dispersion. Larger particle size improves dispersion. This could be observed in Figure 1c and 1d with same filler loading but with larger filler particles. The reason behind this is smaller size has more van der Waals force between the particles compared to larger particles and that decrease the dispersion capability. The particle–particle interaction is high for smaller size and the applied ultrasonic

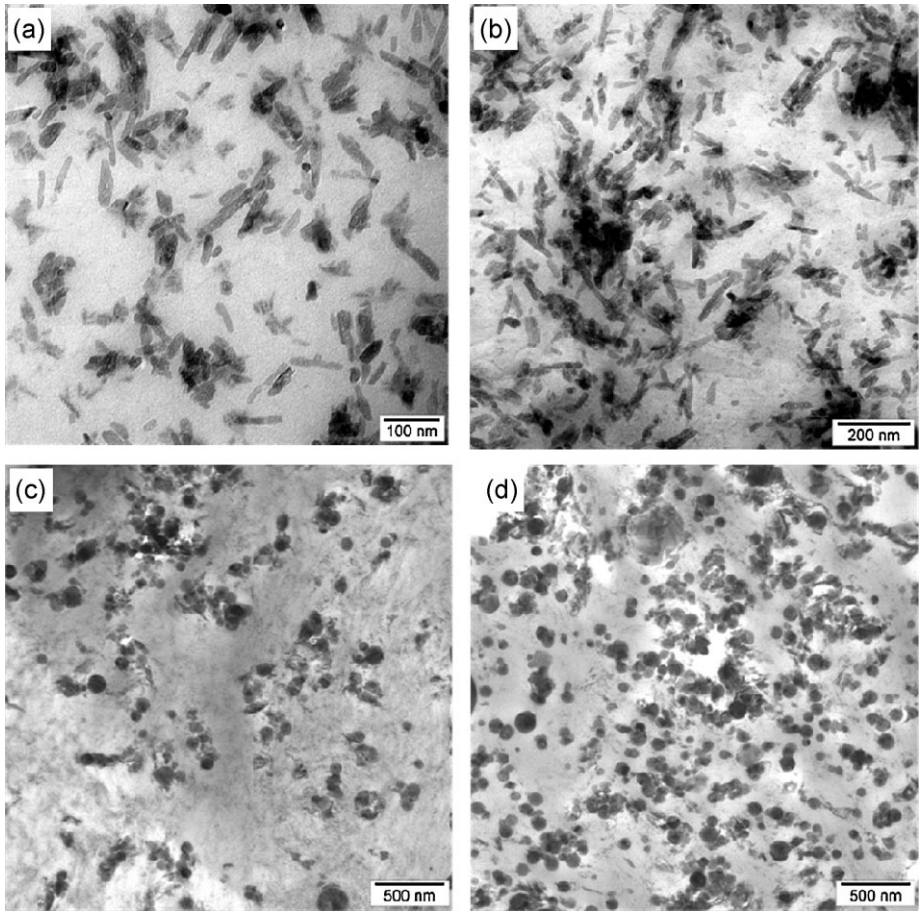

Figure 1.
TEM micrographs of PHB/HA and PHBHV/HA nanocomposites. Samples were cryo-ultramicrotomed and stained with RuO_4. a) PHB/HA (needle) (90/10), b) PHB/HA (needle) (80/20), c) PHBHV/HA (spherical) (90/10), d) PHBHV/HA (spherical) (80/20).

energy and time of dispersion are unable to separate all particle. So, the particles agglomerate and eventually form lumps that we have seen here.

Morphology of Porous Structures Produced by Freeze Drying and Particulate Leaching

Polymer structures with very high porosity and interconnectivity can be obtained by the combination of freeze drying and particulate leaching method. Many of the parameters will influence the structure formation. Polymer concentration has a major contribution in this regard. Concentrated polymer solutions with concentrations higher than 15–20 wt% will not give good pore interconnectivity. In this method polymer solution is forced into sugar/salt templates which have pre-designed pores. This is done by applying very low pressures in the range of 50 to 100 mbar. As the concentration of polymer solution increases, filling up of pores decreases and there is no further interconnectivity. In Figure 2 the modification of pore structures with change in parameters is shown. With decreasing the concentration from 10 to 5% the pore size is nearly doubled, whereas the overall porosity is not altered significantly (Table 1). But when we observe the pure homopolymer with that of filled systems, we can see that the overall porosity is decreasing. Grain size of the particles also influences the pore size. Figure 2 shows SEM micrographs of PHB/HA nanocomposite porous structures. In Figure 2a we can observe the decrease in pore size because the grain size of the salt crystals used are 100–150 μm where as in Figure 2b the grain size of the salt crystals are 200–250 μm. All the other parameters like fusing solution acetone/water 4.5/0.5 w/w, freeze drying conditions and filler loading are kept constant. Every change in parameter will result in different morphology as this process is very sensitive. The pore sizes are relatively small, with a maximum pore size of approximately 60 μm. All scaffolds prepared by freeze-drying and leaching show an irregular porous structure.

However, the final pore architecture achieved has small pore sizes but it has reasonably good interconnection. In Figure 3a it is depicted that the big pore on the surface of the scaffold that is of approximately 70 μm is opened and when imaged below the outer surface we can still observe some small pores inside which shows good interconnection. Nevertheless the pore size are still smaller for osteoblast cells to grow. This limiting value is due to the grain size of the salts and rest of the other parameters influencing in a minute extent.

Porous structures with highly interconnected structures were developed. These

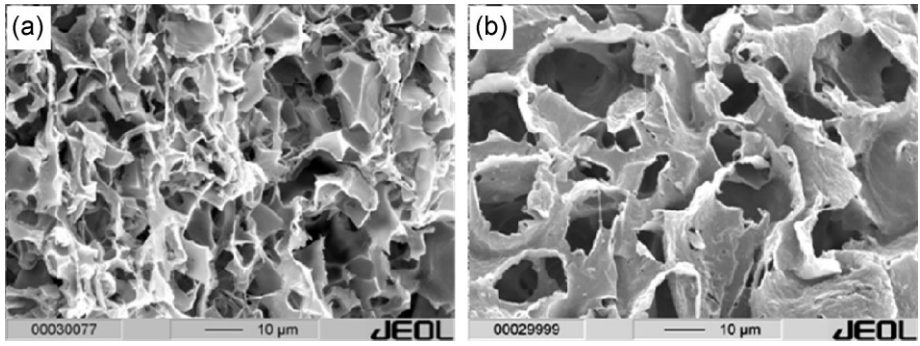

Figure 2.
SEM micrographs of PHB/HA porous nanocomposites prepared by freeze-drying and particulate leaching using salt templates. Larger pores of approximately 50–70 μm result from leaching of salt particles, and smaller pores of approximately 15–35 μm result from freeze drying. a) PHB/HA concentration 10%, grain size of salt template 100–150 μm, and freezing temperature −80 °C; b) PHB/HA concentration 5%, grain size of salt template 200–250 μm, and freezing temperature −80 °C.

Table 1.
Porosities of nanocomposite scaffolds prepared by freeze-drying particulate leaching and melt infiltration techniques.

Polymer	Polymer concentration w/v %	Freezing temperature (°C)	Overall porosity (%)
PHB homopolymer	5	−25	99.35
	10	−25	99.1
	5	−80	99.5
	10	−80	99.3
PHB/HA (90/10)	5	−25	98.79
	10	−25	97.89
	5	−80	98.62
	10	−80	97.5
PHB/HA (80/20)	5	−25	97.32
	10	−25	97.2
	5	−80	97.4
	10	−80	97.2
PCL homopolymer	10		96.4
PCL/HA (90/10)	10		96.1
PCL/HA (80/20)	10		95.3

structures have porosities over 97%. Figure 3a show that highly interconnected porous structures are obtained with large pore sizes of 200–500 μm. This is because the grain size of particles obtained from commercial sugar cubes was much bigger and they were well bound to each other forming a definite pattern of pores with the bigger diameter. When the polymer was forced inside, they retained the morphology of the pores of the sugar cubes. But with leaching and drying, some of the cubes tend to collapse or fuse. Eventually size of pores mainly depends on the size of the grains. As compared with Figure 2 we can observe the pores with smaller diameter with that of Figure 3b. Even though all the parameters were kept constant for both of the samples, only grain size was altered. Polymer concentration and freezing temperature only influence to a lesser extent compared to the grain size. The final pore structure of the scaffolds is determined by the size and content of the sugar particles and also the percent filler introduced in the polymer solution as well as by the solvent-crystal morphology after freezing of the chloroform solution.

Morphology of Porous Structures Produced by Melt Infiltration Technique

Porous structures using melt-infiltration technique show very promising results for PCL scaffolds. Figure 4 presents a comparison of porous structures of PCL

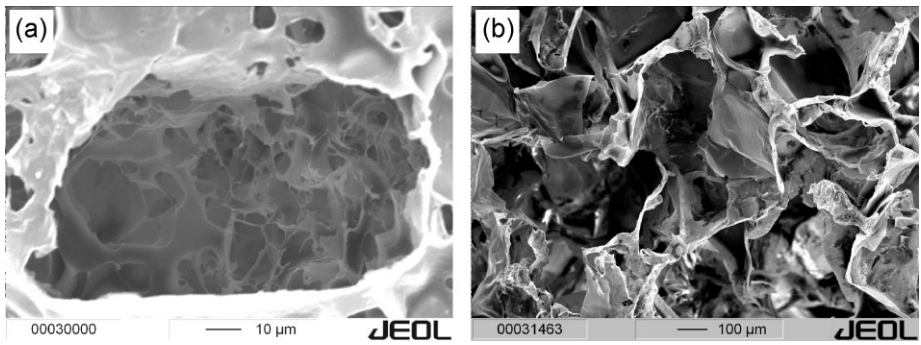

Figure 3.
SEM micrographs of a PHB/HA porous nanocomposite prepared by freeze-drying and particulate leaching polymer nanocomposite/chloroform in the presence of a) salt template and b) in the presence of commercially available sugar template with larger pore sizes of approximately 300–350 μm.

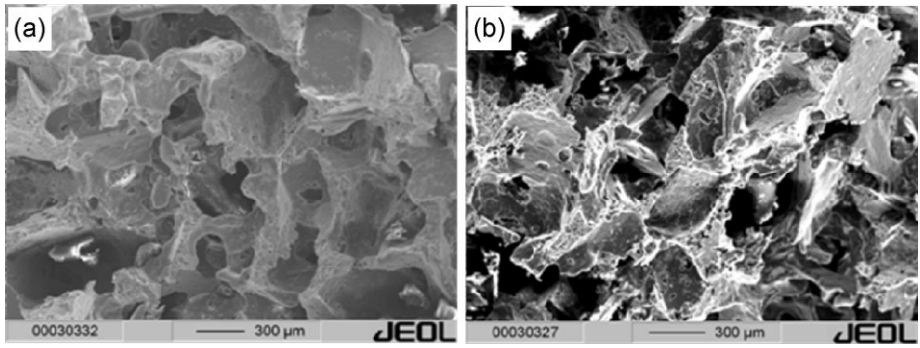

Figure 4.
SEM micrographs of porous structures prepared by melt infiltration technique using sugar templates; a) PCL with 400 um sugar template and b) PCL with 600 um sugar template.

scaffolds prepared using different sugar templates having grain sizes of 400 μm (Figure 4a) and 600 μm (Figure 4b). Both the samples exhibit a very good interconnectivity with pore diameter larger than 300 μm. With increase in grain size from 400 to 600 μm there is a slight increase in pore diameter. In some of the samples there was blocking of pores on the surface; this may be due to the cooling of polymer melt which is above the surface of the templates. Nevertheless, all fractured surfaces display very good porous structures. Polymer infiltration was observed throughout the entire substrate. Table 1 shows the overall porosity of PCL homopolymer as well as composites. Concentration of polymer was kept constant 10w/v %. With the increasing in filler content in the polymer solution there was a slight decrease in porosity. The may be due to dispersion of nanofillers in the interstitial space of the sugar templates, Some of the pores showed smaller diameter compared to other, this may be due to the solidification of the melt before entering into the deeper end of the templates. Temperature of the melted polymer is reduced as it enters into the substrate thus resulting in solidification.

Conclusion

In this work, we were able to prepare nanocomposites of PHB, PHBHV and PCL using two different shaped hydroxyapatite filler. Uniform dispersion of nano fillers were possible even upto 20 wt% filler loading irrespective of shape of the filler. A soncation time of 30 min with 22% (Amplitude) was found to be optimum for good dispersion. Spherical nanoparticles (150–200 nm) showed good dispersion with well separated interparticle distance whereas needle shaped particles (18–30 nm) showed agglomeration due to high vander Waals forces of attraction.

Large porous polymer structures that have very high porosities up to 98% and an interconnected pore network were prepared by freeze drying template leaching and melt infiltration techniques. Results showed very good porous structures with god interconnectivity. Using these techniques it was possible to fabricate 3-dimensional porous structures from the melt as well as solution. The scaffold architecture is determined by the properties of the leachable template, involving the size of the particles employed in the preparation of the templates, the initial concentration of the polymer solution employed in freeze-drying, and the freezing temperature. Larger grain size resulted in pore diameter of about 300–500 μm whereas smaller grain size resulted in pore diameter of 46–70 μm.

The above two method for the preparing of porous polymer structures presented here allows to use both solution

and melt and can be utilized in the biomedical field.

[1] N. A. Peppas, R. Langer, *Science* **1994**, *263*, 1715.
[2] R. Langer, D. A. Tirrell, *Nature*, **2004**, *428*, 487.
[3] J. M. Karp, R. Langer, *Curr. Opin. Biotechnol.* **2007**, *18*, 454.
[4] D. J. Mooney, A. G. Mikos, *Sci. Am.* **1999**, *280*, 60.
[5] J. A. Champion, S. Mitragotri, *Proc. Natl. Acad. Sci. USA* **2006**, *103*, 4930.
[6] J. A. Champion, Y. K. Katare, S. Mitragotri, *Proc. Nat. Acad. Sci. USA* **2007**, *104*, 11901.
[7] J. P. Rolland, et al. Direct fabrication and harvesting of monodisperse, shape-specific nanobiomaterials. *J. Am. Chem. Soc.* **2005**, *127*, 10096.
[8] L. E. Euliss, J. A. DuPont, S. Gratton, J. DeSimone, *Chem. Soc. Rev.* **2006**, *35*, 1095.
[9] Y. Geng, et al. *Nature Nanotech.* **2007**, *2*, 249.
[10] K. H. Roh, D. C. Martin, J. Lahann, *Nature Mater.* **2005**, *4*, 759.
[11] F. Rehfeldt, A. J. Engler, A. Eckhardt, F. Ahmed, D. E. Discher, *Adv. Drug Deliv. Rev.* **2007**, *59*, 1329.
[12] L. E. Nielsen, R. F. Landel, "*Mechanical Properties of Polymers and Composites*", 2nd ed., Marcel Dekker, New York **1994**, Chapt. 7, p. 377ff.
[13] C. Schugens, V. Maquet, C. Grandfils, R. Jerome, P. Teyssie, *Polymer* **1996**, *37*, 1027.
[14] R. Y. Zhang, P. X. Ma, *J. Biomed Mater. Res.* **2000**, *52*, 430.
[15] W. L. J. Hinrichs, E. Lommen, C. R. H. Wildevuur, J. Feijen, *J. Appl Biomater* **1992**, *3*, 287.
[16] J. H. Aubert, A. P. Sylwester, *J. Mater Sci.* **1991**, *26*, 5741.
[17] C. Schugens, V. Maquet, C. Grandfils, C. R. Jerome, P. Teyssie, *J. Biomed Mater. Res.* **1996**, *30*, 449.
[18] S. Gogolewski, A. J. Pennings, *Colloid Polym. Sci.* **1983**, *261*, 477.
[19] R. C. Thomson, M. J. Yaszemski, J. M. Powers, A. G. Mikos, *J. Biomat. Sci. Polym. Ed.* **1995**, *7*, 23.
[20] Y. S. Nam, J. J. Yoon, T. G. Park, *J. Biomed Mater Res.* **2000**, *53*, 1.
[21] K. H. Lam, P. Nieuwenhuis, I. Molenaar, H. Esselbrugge, J. Feijen, P. J. Dijkstra, J. M. Schakenraad, *J. Mat. Sci Mat. Med* **1994**, *5*, 181.
[22] A. G. Mikos, G. Sarakinos, S. M. Leite, J. P. Vacanti, R. Langer, *Biomaterials* **1993**, *14*, 323.
[23] J. H. de Groot, A. J. Nijenhuis, P. Bruin, A. J. Pennings, R. P. H. Veth, J. Klompmaker, H. W. B. Jansen, *Colloid Polym. Sci.* **1990**, *268*, 1073.
[24] C. J. Spaans, J. H. de Groot, V. W. Belgraver, A. J. Pennings, *J. Mat. Sci. Mat. Med.* **1998**, *9*, 675.
[25] A. P. Pego, A. A. Poot, D. W. Grijpma, J. Feijen, *J. Biomat. Sci. Polym. Ed.* **2001**, *12*, 35.
[26] PCT WO 99/25391 (**1999**) invs.: C. E. Holy, M. S. Shoichet, J. E. Davies.
[27] Y. Doi, "*Microbial Polyesters*", VCH Publishers, New York **1990**.
[28] V. Hasirci, in "*Biomaterials and Bioengineering Handbook*", D. L. Wise, Ed., Marcel Dekker, New York **2000**, p. 141ff.
[29] A. El-Hadi, R. Schnabel, E. Straube, G. Müller, S. Henning, *Polymer Testing* **2002**, *21*, 665.
[30] Q. P. Hou, D. W. Grijpma, J. Feijen, *Biomaterials* **2003**, *24*, 1937.

